

Article

Influence of the Applied WC/C and CrN + WC/C Coatings on the Surface Protection of X2CrNi18-9 Cavitation Generators

Wojciech Borek ^{1,*}, Tomasz Linek ², Tomasz Tański ¹ and Perumal Sureshkumar ³

¹ Department of Engineering Materials and Biomaterials, Silesian University of Technology, 18A Konarskiego Street, 44-100 Gliwice, Poland; tomasz.tanski@polsl.pl

² Cerrad Sp. z o.o., ul. Radomska 49B, 27-200 Starachowice, Poland; t.linek@cerrad.com

³ Department of Mechanical Engineering, Ramco Institute of Technology, Rajapalayam 626117, India; sureshkumarp@ritrjpm.ac.in

* Correspondence: wojciech.borek@polsl.pl

Abstract: The purpose of this paper is to investigate the impact of the applied WC/C and CrN + WC/C protective coatings applied using various PVD methods as protection for cavitation generators operating in an environment of intense cavitation wear. In order to carry out planned tasks, special devices generating a cavitation environment have been designed and manufactured. As part of this study, an analysis of the surface of cavitation generators, both before applying the coatings and with the applied protective PVD coatings, and also before and after operation in a cavitation environment, was carried out using the following research techniques: stereoscopic microscopy, scanning electron microscopy, transmission microscopy, XRD, and confocal microscopy. Despite the use of corrosion-resistant steels as a result of the cavitation environment, this causes surface material wear, especially in the area of the through holes. This is due to the fact that there are no protective coatings inside the through hole. Moreover, it was found that, for the tested steel with multilayer CrN + WC/C coatings, there were significantly fewer cavitation defects both on the surface of the material and on the edge of through holes, which indicates that the use of these multilayer coatings can significantly extend the service life of structural elements operating in such environmental conditions. Based on the conducted research tests, it was proven that the applying protective coatings significantly reduce the wear of the surfaces of the tested cavitation generators, thus allowing the use of cheaper steels, not resistant to corrosion, e.g., P265GH steel, which is five times cheaper than austenitic steel. The P265GH steel is used for structural elements in the heating, petrochemical, energy, food, and chemical industries, as well as for structural elements in the aviation, shipbuilding, and many other industries, and, thus, it is possible to reduce the costs associated with the operation of this construction solution in industrial conditions.

Keywords: coatings; PVD; CrN + WC/C; WC/C; cavitation; hardness; wear



Academic Editors: Raimundas Rukūiža and Juozas Padgurskas

Received: 26 November 2024

Revised: 11 January 2025

Accepted: 12 January 2025

Published: 15 January 2025

Citation: Borek, W.; Linek, T.; Tański, T.; Sureshkumar, P. Influence of the Applied WC/C and CrN + WC/C Coatings on the Surface Protection of X2CrNi18-9 Cavitation Generators. *Coatings* **2025**, *15*, 87. <https://doi.org/10.3390/coatings15010087>

Copyright: © 2025 by the authors. Licensee MDPI, Basel, Switzerland. This article is an open access article distributed under the terms and conditions of the Creative Commons Attribution (CC BY) license (<https://creativecommons.org/licenses/by/4.0/>).

1. Introduction

In the process of designing individual machine components or entire devices, prioritizing the durability of the working elements is essential. Engineers should rigorously assess the risks of damage from various forms of friction and wear, such as mechanical wear, fatigue, adhesion, and abrasion, while also considering non-friction-related damage like corrosion, diffusion, cavitation, erosion, and ablation. By addressing these factors comprehensively, we ensure the longevity and reliability of our engineering solutions [1].

When evaluating the mechanisms discussed earlier, it is important to focus on the often-overlooked aspects of cavitation erosion and wear in engineering design. Cavitation occurs when gas bubbles in a liquid implode, a process triggered by rapid pressure drops. This phenomenon generates shock waves measuring 0.1 to 0.2 mm in length and traveling at speeds reaching several hundred meters per second. Unfortunately, these shock waves can damage the surfaces of components, resulting in the formation of deep pits and craters [2,3]. To enhance the resistance of water flow systems—such as pumps and supply networks—against cavitation wear, we must consider the choice of materials and their surface treatments, properties, and microstructures. Cavitation pits are often found on structural elements, particularly near scratches and surface defects that may occur during manufacturing. These imperfections can arise accidentally during transport or maintenance, or due to lapses in operation [3]. In the context of fluid transportation, especially for water, reliability can be significantly impacted by cavitation wear on flow system components. This is particularly true for rotodynamic single- or multi-stage pumps utilized in water supply stations and systems, as well as components of water turbine blades [4]. A proactive approach to mitigate cavitation effects includes selecting materials known for their resistance to cavitation wear in medium transportation applications. Employing stainless and acid-resistant steels, as well as alloys like bronze and brass, can greatly improve the longevity and reliability of water supply systems and pumps. By focusing on these effective materials, we can build more resilient systems that withstand the challenges posed by cavitation [1–7].

Cavitation erosion is a significant concern that goes beyond isolated cases in water distribution or electricity generation, particularly in the operation of turbines within hydropower plants. Its effects are felt throughout the entire water transportation infrastructure, various types of power and heating systems, and facilities involved in electrical energy production, including combined heat and power plants that deliver both electricity and thermal energy. Additionally, municipal heat distribution plants and all systems that supply thermal energy in the form of steam or water are impacted by this issue. Since the power sector, heat distribution sector, and heating sector are vital and strategic pillars of any nation's economy, potential failures in these areas can lead to considerable financial losses. Therefore, it is crucial that we urgently address the challenge of cavitation erosion and wear in these essential sectors [8].

The heating and heat distribution sectors are exploring cavitation processes to improve the heating of carriers, such as circulating water in central heating systems. A key example is the cavitation pump, which converts mechanical energy into thermal energy through centrifugal flow-based heating. This technology is primarily used in residential heating systems in the United States and Australia [1,2,5–7]. However, the challenges posed by the cavitation effect and its associated wear necessitate further scientific and industrial research. Recognizing the need for continued investigation underscores the importance of advancing the field and encourages stakeholders to deepen their understanding of cavitation wear and the degradation of engineering materials [3,4,8].

In order to protect structural components from undesirable external conditions responsible for damage, various types of surface engineering techniques are very often employed, with vacuum technologies in many cases, which include physical vapor deposition (PVD) techniques. Physical vapor deposition (PVD) is a vaporization coating technique that involves the transfer of material at the atomic level. In the first step of the process, the material to be deposited on the structural element is converted into vapor by physical means such as high temperature, vacuum, or gas plasma. The vapor is then transported to a low-pressure area from the source to the substrate, condensing on the substrate to form a thin layer. PVD processes deposit films with thicknesses ranging from a few nanometers to

thousands of nanometers. However, they can also be used to create multilayer coatings [9]. These methods allow a thin protective coating to be deposited on a coated component to counteract tribological and non-tribological wear. As a rule, they are applied on the surface of materials with reduced mechanical strength and corrosion resistance in relation to the expected ones. The surface and/or top layer is, in most cases, responsible for the properties of individual elements as well as entire systems. Modern surface engineering technologies, including PVD techniques, allow for the protection of the surface of engineering material effectively enough to change its functionality, e.g., to increase its corrosion resistance, and mechanical and/or physicochemical and decorative properties for use as a constructional element [9–11].

Furthermore, PVD-applied coatings are characterized by a high hardness, oxidation resistance, and low coefficient of friction. Due to the fact that most of the machine components and industrial equipment during their operation are continuously exposed to mechanical impact and fatigue loads operating in a variable, undefined, and indescribable cycle, the knowledge of the PVD coatings' degradation mechanisms under dynamic load is particularly important. Therefore, analyzing the effect of applied protective coatings on the cavitation wear resistance properties of structural components operating in a hydrodynamic environment is an important engineering issue presented in this paper [11–14].

Research on the cavitation wear resistance of austenitic steels has been carried out on a large scale in many research centres worldwide and has been described in many scientific publications [2–4,7–19]. As proven in the research, among the frequently used austenitic steels, the Hadfield grade is characterized by the highest cavitation wear resistance compared to the cavitation wear resistance of AISI 304 (American Iron and Steel Institute) (X5CrNi18-10) and AISI 316 (X5CrNiMo17-12-2) steels. The X5CrNi18-9 steel exhibits much higher cavitation resistance than Hadfield steels when we take into account their surface hardnesses, which is, respectively, about ~215 HB and ~500 HB. This advantage can be attributed to the relatively high yield strength $R_{p0.2}$ in the range of 220–350 MPa of these steels. In AISI 304 (X5CrNi18-10) and AISI 316 (X5rNiMo17-12-2) austenitic steels and Hadfield steel, the weight loss is due to the initiation and propagation of slip bands, twin boundaries, and grain boundaries. In Hadfield's manganese steel, the phenomenon of material spalling occurs, also between the slip lines of the microstructure. In each of the cases considered above, the advanced degree of cavitation wear can contribute to the ductile fracture of the sample, which may indicate the high impact strength of the material [9]. Based on cavitation tests on a rotating disc bench, it was shown that the cavitation resistance of Fe-Mn-Si and Fe-Cr-Ni-Mn austenitic steels does not correlate strongly with the hardness of their surfaces but depends on their elasticity and the alloy's ability in strain hardening [17–26].

The main purpose of this paper is to investigate the impact of the applied WC/C and CrN + WC/C protective coatings applied using various PVD methods as protection for cavitation generators manufactured from X2CrNi18-9 steel which were operating in an environment of intense cavitation wear.

2. Research Material and Methodology

X2CrNi18-9 steel, whose chemical composition, according to PN-EN 10088 standard, is presented in Table 1, was used in this study. This steel belongs to the group of corrosion-resistant steel; it is chromium-nickel X2CrNi18-9 steel with an austenitic structure. X2CrNi18-9 steel is used, among other things, for the production of equipment, apparatus, and fittings in the chemical, petrochemical, food, and energy industries, and responsible structural elements in the railroad, aerospace, and shipbuilding technologies.

Table 1. Chemical composition of the austenitic stainless steel X2CrNi18-9 by PN-EN 10088 tested in the conditions of cavitation wear [mass fraction, %].

C, %	Mn, %	Si, %	Cr, %	Ni, %	N, %	S, %	P, %
0.03	2.0	1.0	18	9	0.1	0.02	0.01

An important issue in this study was the selection and qualitative and quantitative optimization of low-friction and anti-wear composite coatings applied by physical vapor deposition (PVD) to protect the surface of steel generators against cavitation wear. On the basis of literature data as well as the data obtained on the properties of commercial coatings, two coatings, i.e., CrN and WC/C, were selected for this study. The CrN coating was selected due to its high corrosion resistance, similar to that provided by chromium plating technologies. Moreover, the CrN coating is characterized by the following: resistance to fluorides, chlorides, and other corrosive substances, high adhesion and hardness, very high corrosion resistance, and low coefficient of friction. The CrN coating was manufactured according to the proprietary technology developed by Oerlikon Balzers Coating Poland Sp. z o.o., using the ARC-PVD cathodic arc evaporation method. The WC/C coating has a very low friction coefficient and good sliding properties, which translates into high resistance to fatigue wear and surface tribooxidation. The WC/C coating is a typical tribological layer which is used to reduce adhesive wear associated with, for example, seizures. The WC/C coating was deposited by pulsed reactive magnetron sputtering at Oerlikon Balzers Coating Poland Sp. z o.o. At this point, I would like to emphasize that, as part of this work, PVD coatings were applied by a private company, Oerlikon Balzers Coating Poland Sp. z o.o., which specializes in PVD technology and, depending on the substrate material, has precisely developed parameters for the coating application process. The method of coating application itself was not the basis for research in this publication; this is the know-how of Oerlikon Balzers Coating Poland Sp. z o.o. To simplify the description of the test results, the cavitation generator made of X2CrNi18-9 steel with PVD-deposited WC/C coating is denoted as X1, while the cavitation generator with CrN + WC/C coating is designated as X2, and, without any coatings, X.

In order to carry out planned tasks, special devices generating a cavitation environment have been designed and manufactured. Based on more than 10 years of experience in the heating and district heating industry, the author's own thoughts, and the application of structural and technological solutions, an original test stand was designed, constructed, and put into operation as a research and measurement system for the process and continuous generation of a cavitation environment. The cavitation environment was obtained through a pump forcing water flow, in which the designed cavitation generator was installed. The constant parameters in the test and measurement system were water flow at a constant temperature of about 40 °C and stabilized pressures upstream (240 MPa) and downstream (50 MPa) of the cavitation medium, controlled by manometers. Each time during the implementation of the sample, the test and measuring system operated in continuous motion and in a closed cycle (closed water circuit) for 500 Productive Machine Hours (PMHs) corresponding to 21 working days (working month), referring to the 3-shift work system practiced in industrial plants. After 500 PMHs at the end of the operation of a given cavitation generator, the research and measurement system was, each time, cleaned and flushed with running water. The detailed scheme of the device (Figure 1a), as well as the optimization of the generator shape and the results of numerical computer simulation using Computational Fluid Dynamics (CFD) technique with ANSYS FLUENT software are presented in the earlier publications of the authors of this paper [13–19]. Figure 1 shows a real photo of the cavitation generator without protective coating and the installation

method of the cavitation generator, along with the marking of the water flow direction in the research and measurement system in the author's closed-cycle continuous flow device operating for 500 PMHs generating a cavitation environment.

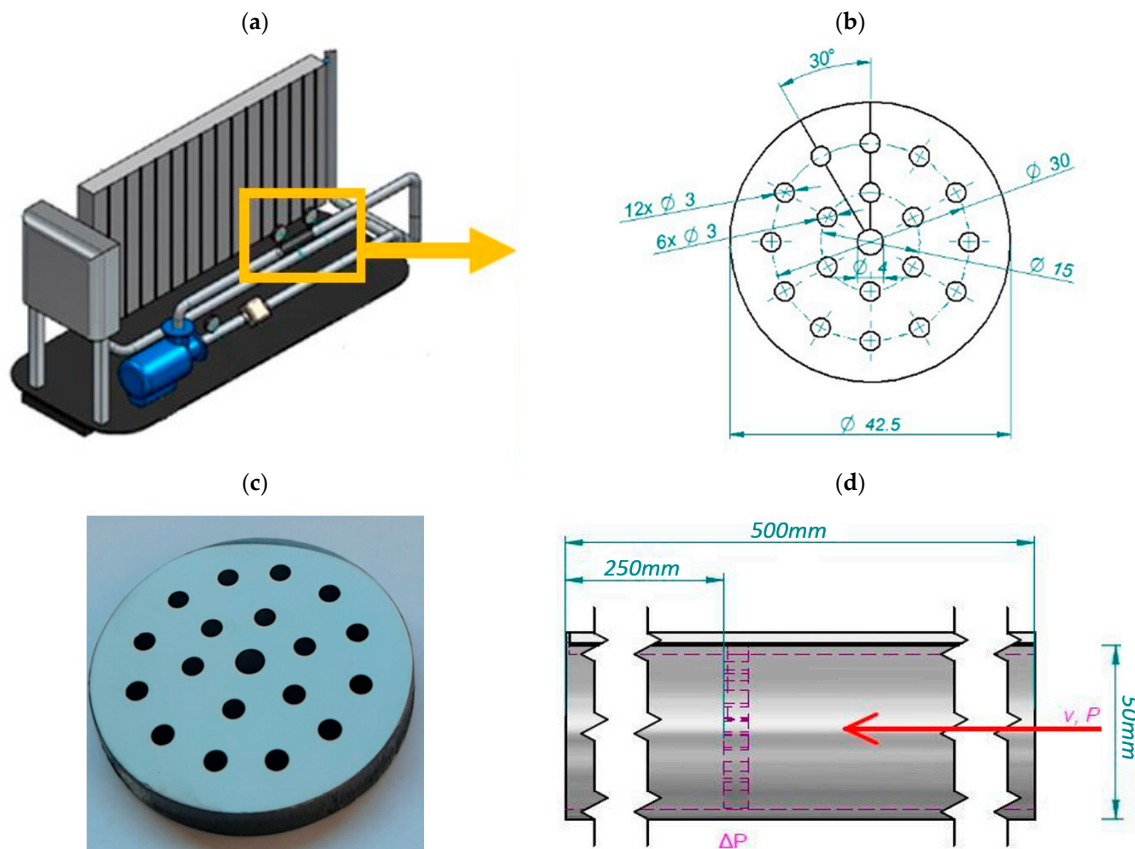


Figure 1. Model of a stream and flow device generating a cavitation environment; (a) isometric diagram of the device, and testing and measuring system; (b) cavitation generator model's dimensions and shape, with thickness of cavitation generator—5 mm; (c) representative view of the structural element used as a cavitation generator; and (d) location in the place where the cavitation environment was formed—the red arrow indicates the direction of water flow.

A cavitation generator without a PVD protective coating was also operated under the conditions of cavitation wear in a stream and flow device continuously for 500 PMHs in order to investigate the influence of these operating conditions on the base material.

The results of macroscopic examinations of investigated steel without PVD coatings after cavitation wear conditions were made with a stereoscopic microscope, Stereo Discovery V12, by Zeiss (Carl Zeiss, Jena, Germany), with a magnification of 8 to 100 \times . In addition, structure observations of tested generators with and without PVD coatings were made on a ZEISS SUPRA 35 scanning electron microscope at an accelerating voltage from 5 to 20 kV using secondary electron detection (SE).

Nanohardness tests and Young's modulus determination of WC/C and CrN + WC/C coatings before the operation was carried out on a FISCHERSCOPE HM2000 XYp apparatus from HELMUT FISCHER (Sindelfingen, Germany) using WIN-HCU software (version 2022) in accordance with DIN EN ISO 14577-1. The measurements were made using the Martens method with the following settings:

- Confidence level (measurement error) in the range of 6 to 164;
- Indenter penetration rate in the range: 0.125/20–0.250/20 $\mu\text{m/s}$;
- Coefficient of variation ranging from 4.2 to 12.0%;

- Standard deviation: 5–156.

Five nanohardness measurements were performed for each cavitation generator. Young's modulus was determined using the load–unload method consisting of displacement of a diamond ordinary Berkovich indenter under load deep into the tested material to a depth of 10% of the total thickness of the tested coatings.

Phase composition studies were performed in a Panalytical X'Pert PRO MPD X-ray diffractometer (Malvern Panalytical Ltd., Malvern, UK) equipped with a cobalt anode X-ray tube ($\lambda K\alpha = 0.179$ nm) and a PIXcel 3D detector. Diffractograms were recorded in Bragg–Brentano geometry in the 30–110° 2Theta angle range with a step of 0.026° and a counting time per step of 100 s. In addition, X-ray qualitative phase analysis was performed using HighScore Plus software (v. 3.0e) and the dedicated PAN-ICSD inorganic crystal structure database.

Thin films for structural studies on FEI's TITAN 80-300 high-resolution transmission electron microscope (FEI, Hillsboro, OR, USA) were prepared using the Focused Ion Beam (FIB) technique on a Hitachi FB-2100 FIB microscope (Hitachi High-Tech Europe GmbH, Germany) and FEI Helios NanoLab™ 600i SEM/Ga-FIB. Structural and diffraction studies were performed on an FEI Titan 80-300 S/TEM microscope at 300 kV equipped with a CMOES beam collector for scanning transmission electron microscope (STEM) operation and an Edax EDS spectrometer (Thermo Fisher Scientific Inc., Waltham, MA, USA). Research techniques such as brightfield (BF), darkfield (DF), high-resolution TEM, high-resolution image (HRTEM), and energy-dispersive X-ray spectrometry (EDS) were used for structural and diffraction analysis of the studied steels.

Detailed analysis of the topography of the investigated cavitation generators was performed using the confocal laser scanning microscopy (CLSM) technique on a ZEISS Exciter instrument with the ZEN software package (version 2020), which allows a series of images to be superimposed into a single three-dimensional co-focal (confocal) package at a measurement range of 10 to 130 μm .

3. Research Results

The result of the macroscopic examinations of X2CrNi18-9 steel without PVD coatings in cavitation wear conditions made with a stereoscopic microscope is shown in Figure 2. A few places in the X2CrNi18-9 cavitation generator were identified based on macroscopic photographs, especially near the edges of the straight-through openings, where cavitation corrosion was initiated. In addition, axial brittle cracks going deep inside the material were also identified, initiated with an eroded edge of the straight-through opening.

On the basis of detailed structural investigations of the surface of the examined X2CrNi18-9 steel in the pre-operational condition with WC/C and CrN + WC/C coatings applied on their surface (marked X1 and X2, respectively), using a scanning electron microscope, it was found that the surface morphology of the WC/C coatings is characterized by high inhomogeneity related to the occurrence of numerous solidified droplet-shaped microparticles (Figure 3). The occurrence of these defects is a characteristic drawback of the PVD process; these droplets are formed during the cooling of the substrate surface, after the coating application process. The WC/C droplets formed vary in size, ranging from tenths of a micrometer to several micrometers. The average thickness values of the individual coatings were also determined from the breakthrough studies of the cavitation generators (Figure 4). The WC/C coating thickness for the cavitation generator designated X1 is 1.95 ± 0.03 μm , while, for the X2 generator, the CrN thickness is 1.12 ± 0.03 μm and WC/C was 0.90 ± 0.03 μm . The total CrN + WC/C coating thickness for the X2 cavitation generator was 2.02 ± 0.06 μm .

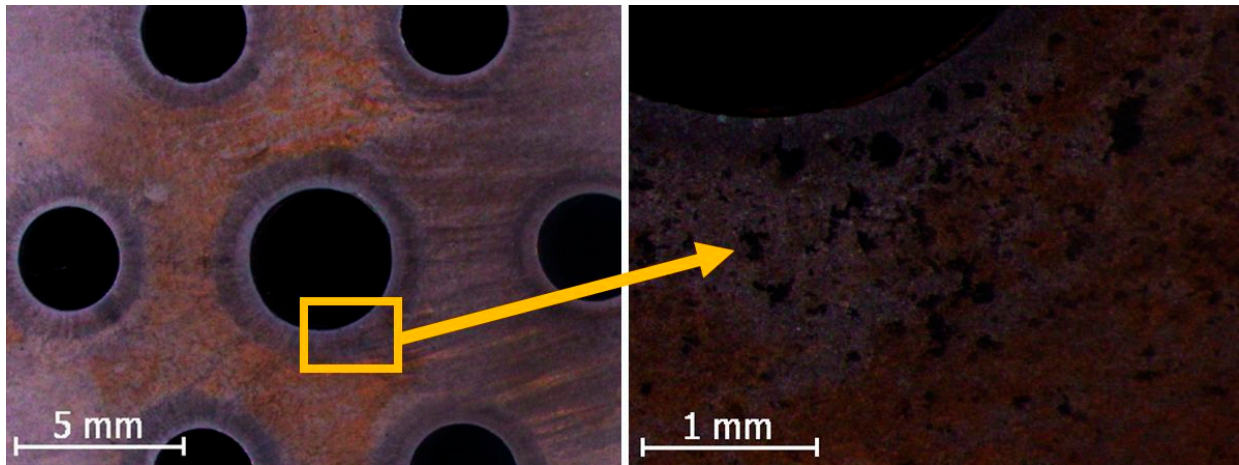


Figure 2. Result of cavitation wear of the surface of a constructional element made of X2CrNi18-9 steel after operation in a stream and flow device for 500 PMHs.

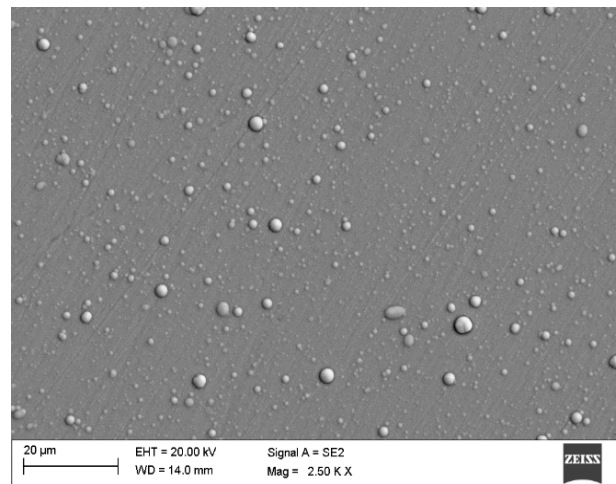


Figure 3. Surface topography of WC/C coating applied to steel X2CrNi18-9.

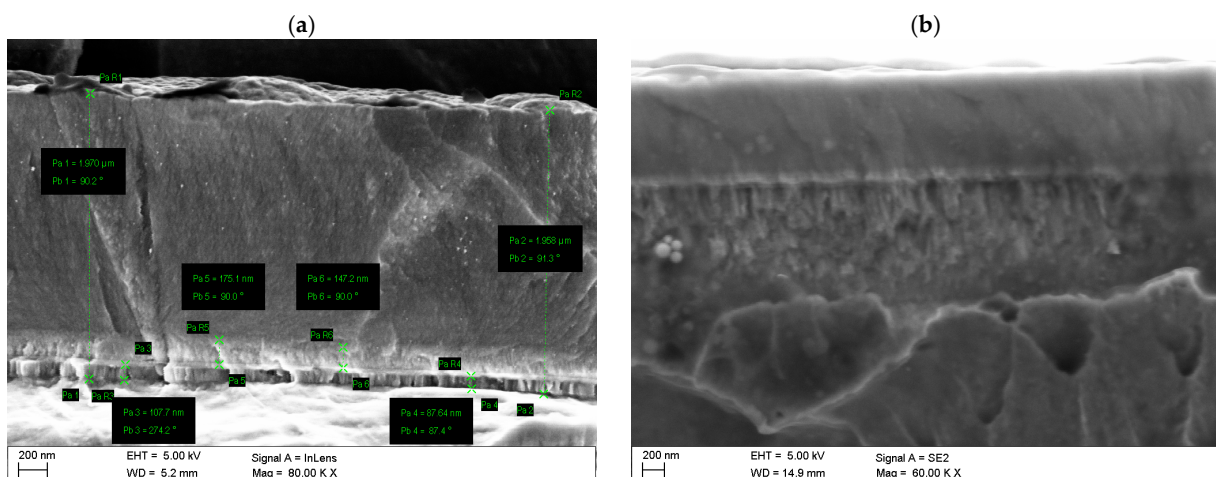


Figure 4. Fracture surfaces of PVD deposited coatings: (a) X1 and (b) X2.

In order to characterize the mechanical properties of the applied coatings, nanohardness tests were performed for the applied PVD coatings. Based on the tests performed, it was found that the nanohardness of the WC/C protective coating for the cavitation generator marked X1 is 13 GPa, while, for the X2 generator, it is higher by about 2 GPa or

about 15%. The results of Young's modulus measurements for the WC/C coating for the two tested cavitation generators X1 and X2 are 133 and 123 GPa, respectively.

Based on the results from the qualitative X-ray phase analysis, the diffraction lines coming from the crystalline planes were confirmed; i.e., in the initial state, the X steel is characterized by an austenitic structure, which is approved by the peaks coming from the phase Fe γ (Figure 5). A qualitative X-ray phase analysis of cavitation generators, with an applied protective coating, both before and after operation in the flow-blasting device, for the X steel tested, did not confirm the occurrence of distinct peaks for the phases originating from the applied coatings, i.e., CrN and WC/C. On the X-ray diffractograms, there was only a broad/fuzzy diffraction line, the so-called broadening, resulting from the diffraction of the X-ray beam on the amorphous structure, in the angular range between $35 \div 50^\circ 2\theta$ (Figure 5). In order to verify the results obtained from the qualitative X-ray phase analysis of the investigated cavitation generators with CrN and WC/C coatings, the diffraction technique was applied at a fixed incidence angle of the primary X-ray beam using a parallel beam collimator in front of a proportional detector. The studies were performed in a fixed incidence angle geometry α equal to 1.5 and 3° . The studies at a fixed incidence angle of the primary beam did not allow the registration of reflections from thin surface layers, which proves the amorphous nature of these PVD-applied coatings. The results of these studies were also confirmed in the study of thin films on a high-resolution transmission microscope and are presented later in this paper.

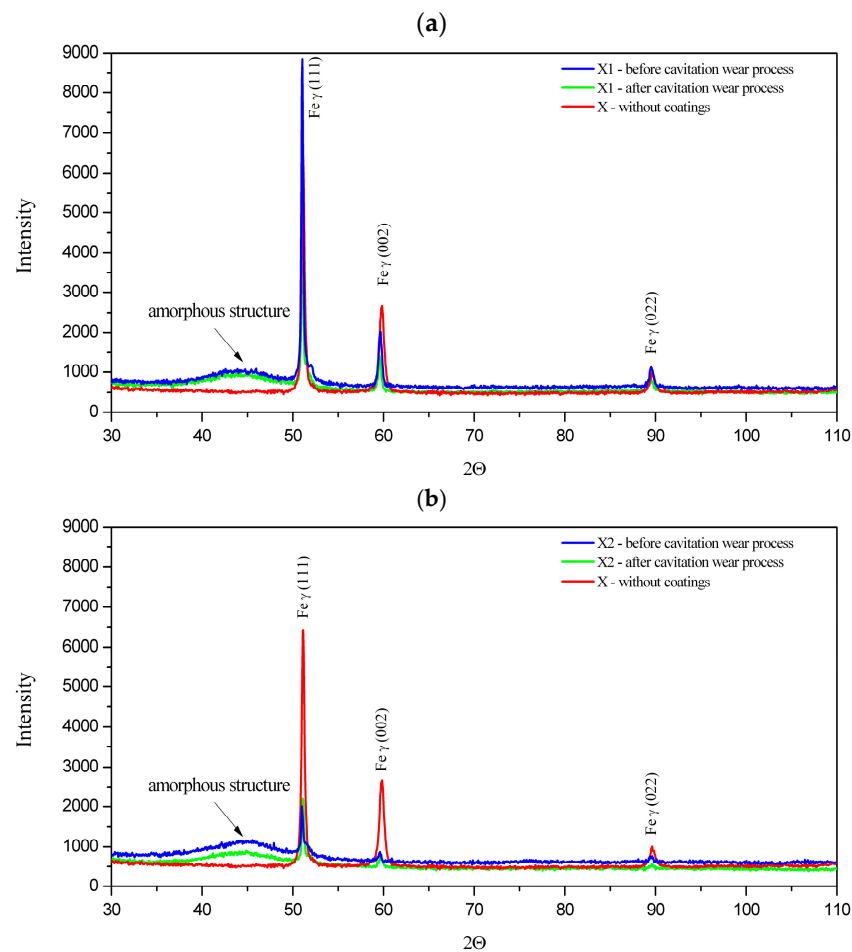


Figure 5. X-ray diffractograms of investigated cavitation generators without and with WC/C (a) and CrN + WC/C (b) coatings before and after operation in a flow-blasting device.

Based on the results of thin films obtained by transmission electron microscopy, the multilayer nature of WC/C and CrN + WC/C coatings was confirmed. The results of tests performed on cross-sections of the X1 cavitation generator confirm the homogeneity of the WC/C coating (Figure 6). The presence of a Cr adhesion sublayer with a thickness of about 50 nm and a CrN + WC/C transition zone between the layers, with a thickness of 25 nm, was also found (Figure 6). Quantitative and qualitative X-ray microanalysis using an EDS confirmed the presence of the main alloying additives Fe, Ni, Cr, and W included in both the substrate and the applied PVD coatings, including the Cr adhesion sublayer (Figure 6f). The results of diffraction studies obtained using a high-resolution transmission electron microscope confirm that, as intended, the substrate of the X1 cavitation generator has an austenitic structure (Figures 6c,d and 7). Based on the results of the X1 cavitation generator substrate obtained by transmission electron microscopy, narrow parallel grains with a width of several to tens of nanometers were visualized (Figure 7). Diffraction studies proved that these are austenite grains oriented in the [011] direction, containing numerous slip bands. The presence of slip bands is also clearly confirmed by high-resolution HRTEM images (Figure 7c,d). Twins were also identified in the studied sample using high-resolution imaging (Figure 7c). The fast Fourier transform (FFT) determined from the area marked in green (Figure 7c) is shown in the upper left corner (Figure 7c). The mirror-like orientation of the reflections is characteristic of the twinning boundary. The mirror-like orientation of the spatial network of the indicated fragment is also visible in Figure 7d. The STEM brightfield images (Figure 7e,f) indicate the presence of slip in two directions (at 60° relative to each other). Both slip bands and twins indicate the deformational strengthening of the studied micro-areas subjected to cavitation stresses. These stresses cause an increase in the density of dislocations interlocking with each other, which is an obstacle to the free sliding motion and, ultimately, leads to the formation of dislocation strands and their pile-up. The result of the described evolution of structure factors is the deformational strengthening of the top layer of the X cavitation generator substrate.

In order to confirm the occurrence of the chemical composition change on cross-sections of individual layers of cavitation generator X2, a linear EDS analysis was performed (Figure 8a,b). Similarly, as in the case of the X1 generator, the presence of a 50 nm-thick Cr adhesion sublayer (Figure 8c) and two transition zones (mixed) Cr+CrN+Cr, CrN+Cr+W with a thickness of 25 nm imaged in the bright- and darkfield (Figure 8) were found. The proportion of transition zones may indicate diffusive areas between the substrate and subsequent layers and sublayers. The generated sublayers provide improved adhesion between the substrate and the coating and between the CrN and WC/C layers, characterized by different physical and chemical parameters. The quantitative and qualitative X-ray microanalysis performed with an EDS confirmed the presence of the main Fe, Ni, Cr, and W alloying additives included in both the X2 cavitation generator substrate and the applied PVD coatings, including the Cr adhesion sublayer and transition zones (Figure 8c–f). Furthermore, the transmission electron microscopy results confirm the amorphous nature of the WC/C coatings, where significant diffraction ring blurring is evident for all cavitation generators investigated: X1 and X2 (Figure 9f).

In order to analyze the effect of the implemented cavitation wear conditions of generators with the applied protective coatings, the surface topography before and after the operation was examined using the laser confocal microscopy technique. Figure 10 shows a representative micro-area of sample X2 before the operation at a location near the through hole. The sample's surface was flat before the tests performed, and there was no distortion at the location of the through hole. After exploitation in the flow-blasting device, the cavitation generator X1 was characterized by a significant difference in the profile height of the tested part of the surface, within 13 μm at the measuring distance of about 20 μm

from the edge of the through hole (Figure 11). The obtained test results illustrate a wide band of material loss, of varying volume, ending at different heights of the working edge of the cavitation generator hole, which confirms the irregular nature of the material failure. In contrast, the cavitation generator marked X2 exhibited a very mild change in the wear profile with a surface height difference of about $2.5\ \mu\text{m}$ over a measurement distance of about $5\ \mu\text{m}$. Only slight irregular material loss was observed at the edges of the working bore (Figure 12).

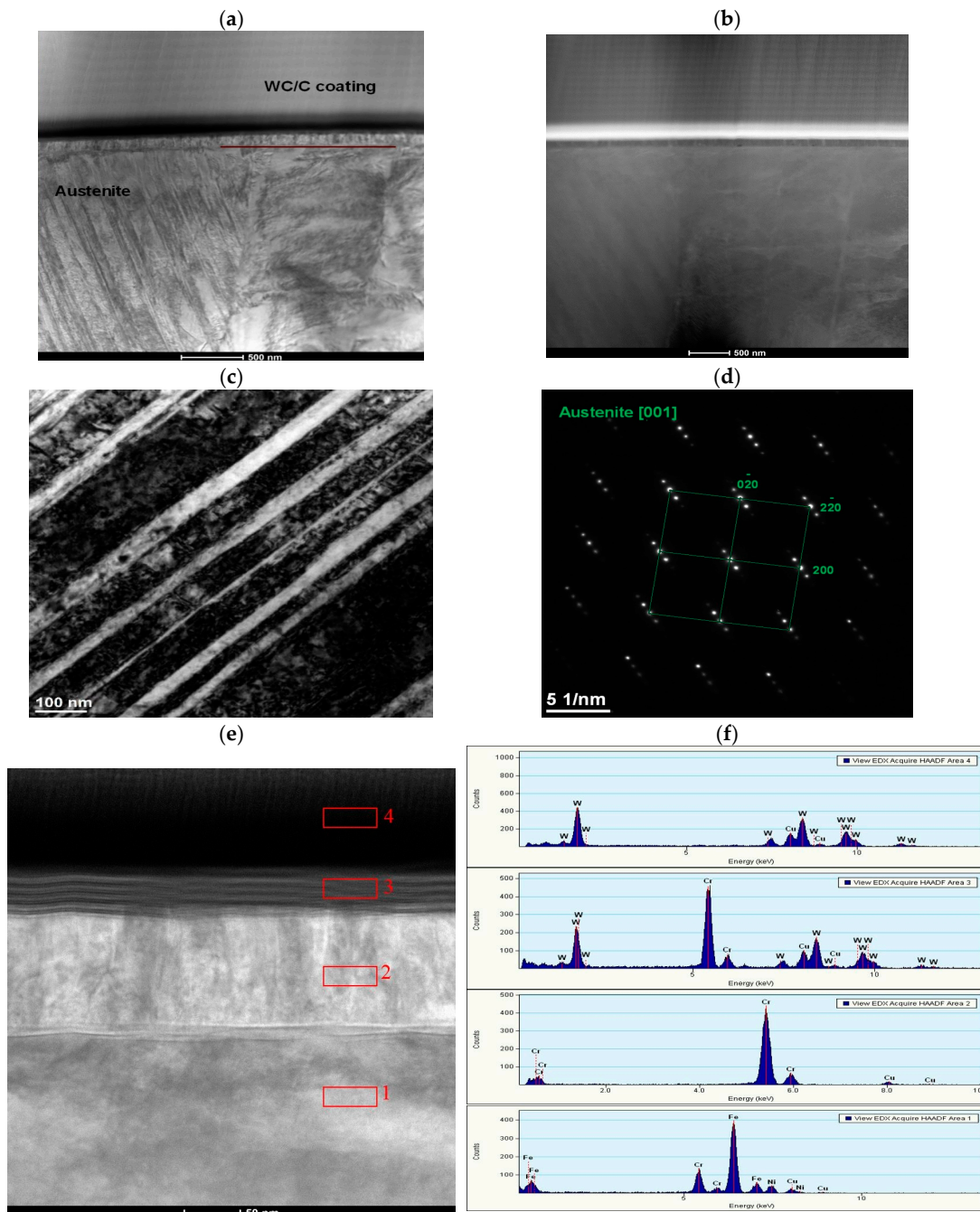


Figure 6. Structure of the X1 cavitation generator: (a) brightfield; (b) darkfield from Figure 6a; (c) substrate brightfield; (d) diffraction from Figure 6c; (e) brightfield; and (f) intensity plots as a function of scattered X-rays from areas 1–4 in Figure 6e, and red rectangle in Figure 6e—examined micro area.

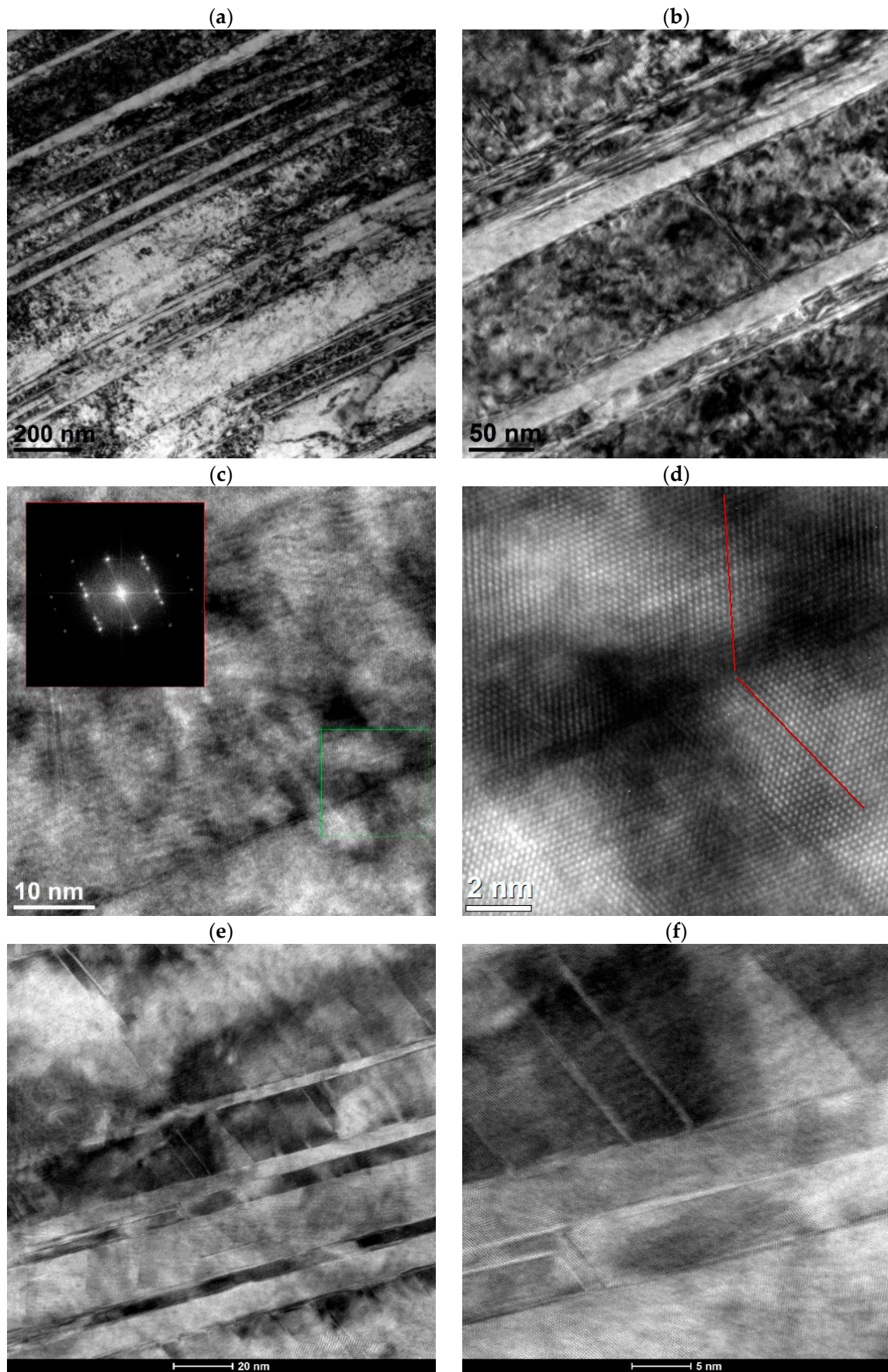


Figure 7. Structure of the X1 cavitation generator substrate: (a,b) TEM brightfield, (c,d) HRTEM, and (e,f) TEM brightfield.

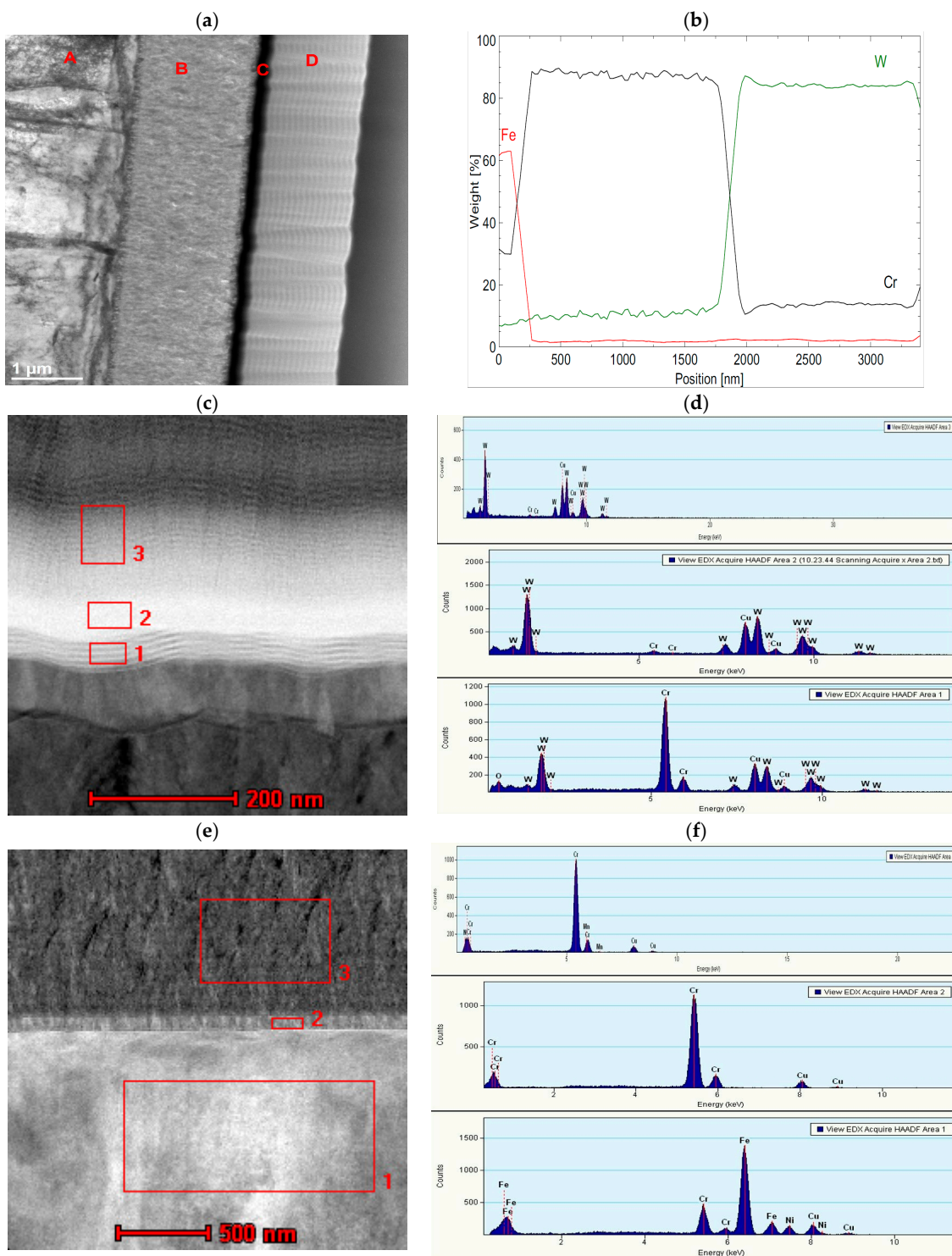


Figure 8. Structure of cavitation generator X2: (a) brightfield; (b) linear analysis of PVD coating elemental distribution from Figure 8a; (c) brightfield (d) intensity plots as a function of scattered X-ray from areas 1–3 in Figure 8c; (e) brightfield; and (f) intensity plots as a function of scattered X-ray from areas 1–3 in Figure 8e; individual coatings in the tested sample are marked with letters A–D.

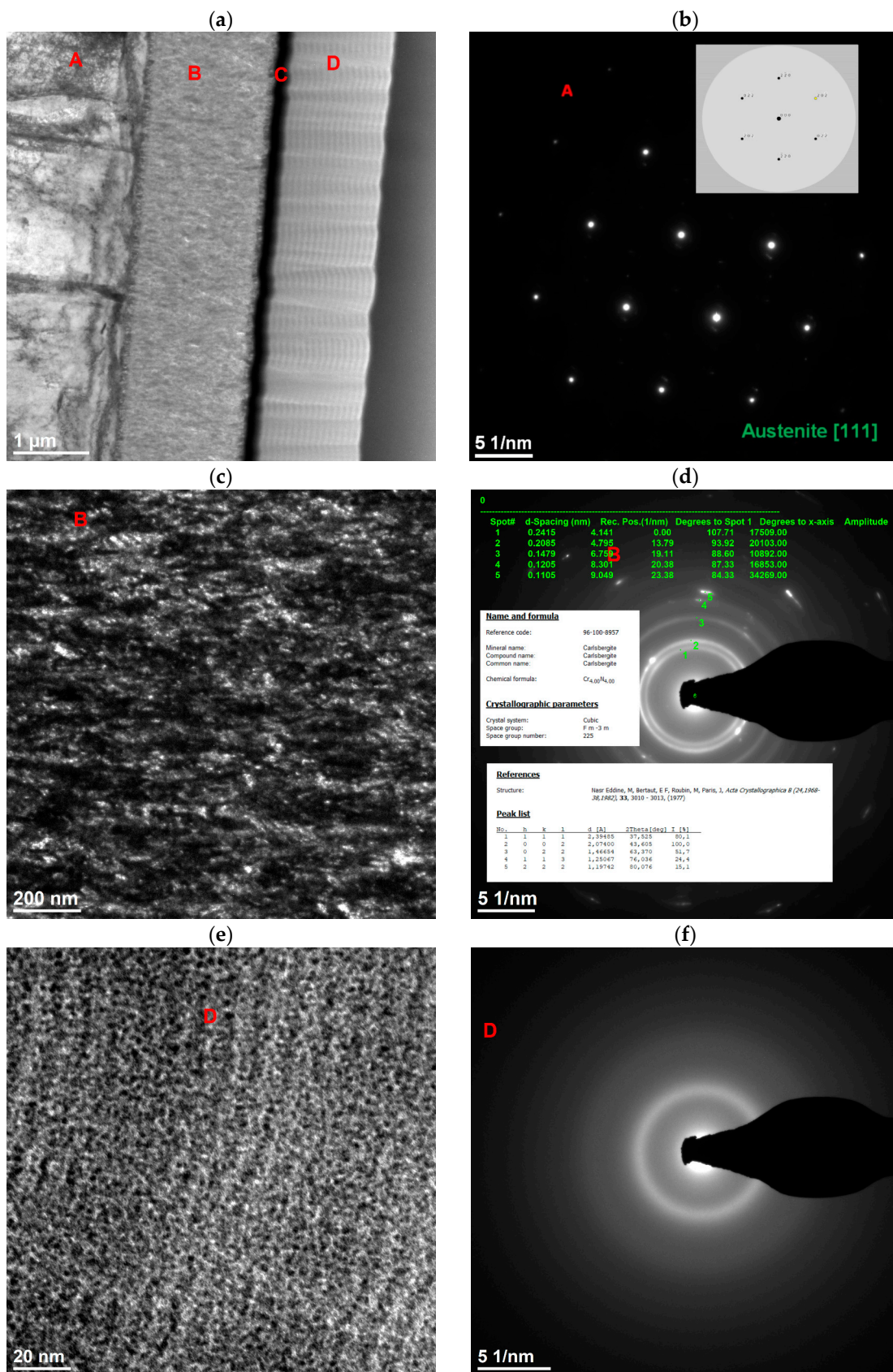


Figure 9. Structure of the X2 cavitation generator: (a) brightfield; (b) diffraction from area A in Figure 9a; (c) darkfield of CrN coating (d) diffraction from Figure 9c; (e) darkfield of WC/C coating; and (f) diffraction; individual coatings in the tested sample are marked with letters A–D.

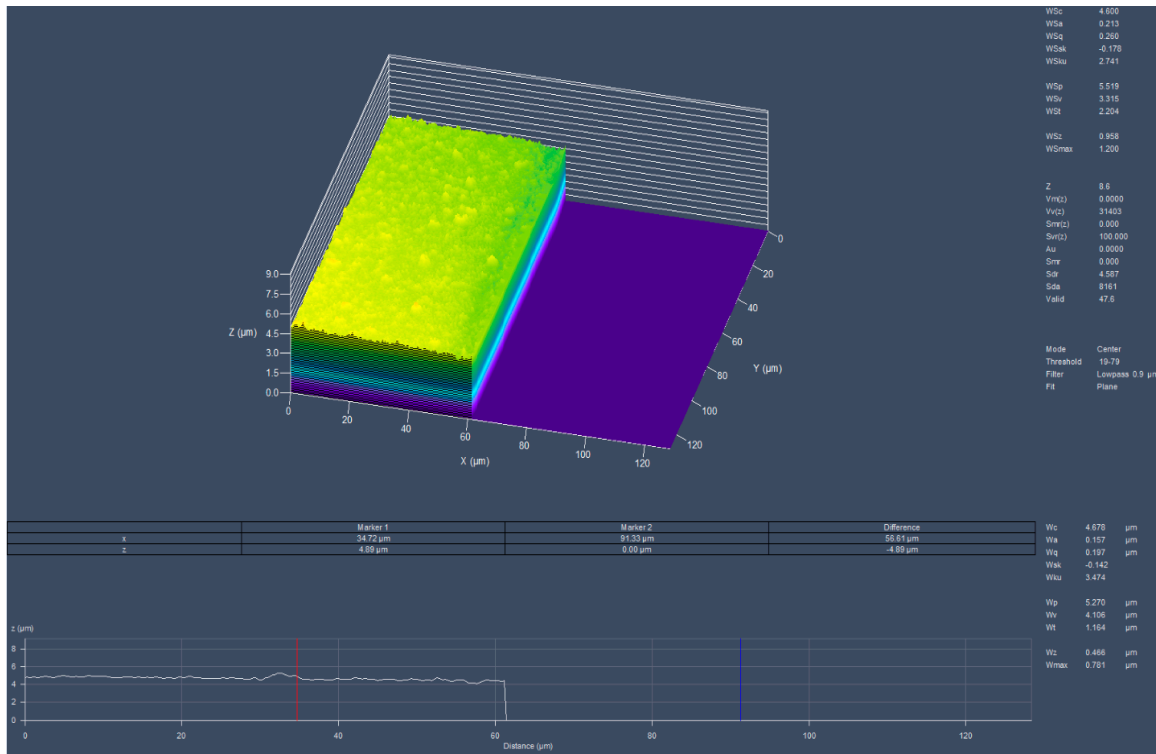


Figure 10. Surface topography of sample X2 before operation; red line—measuring line.

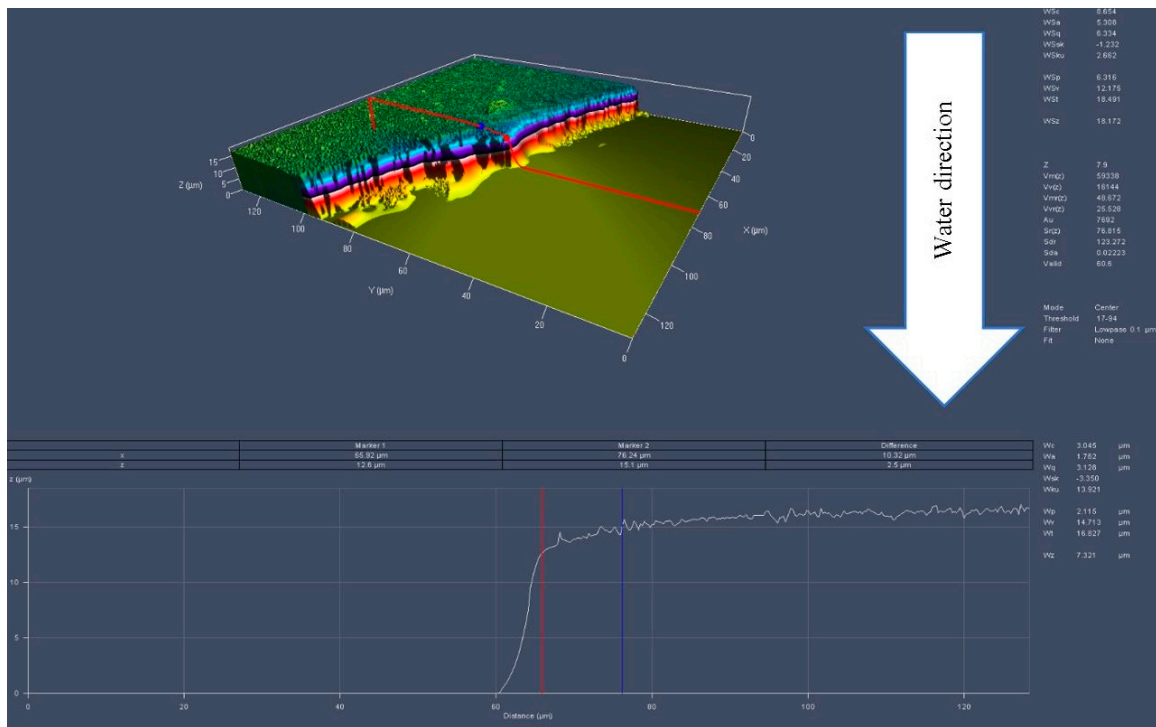


Figure 11. Surface topography of sample X1 after operation; red line—measuring line.

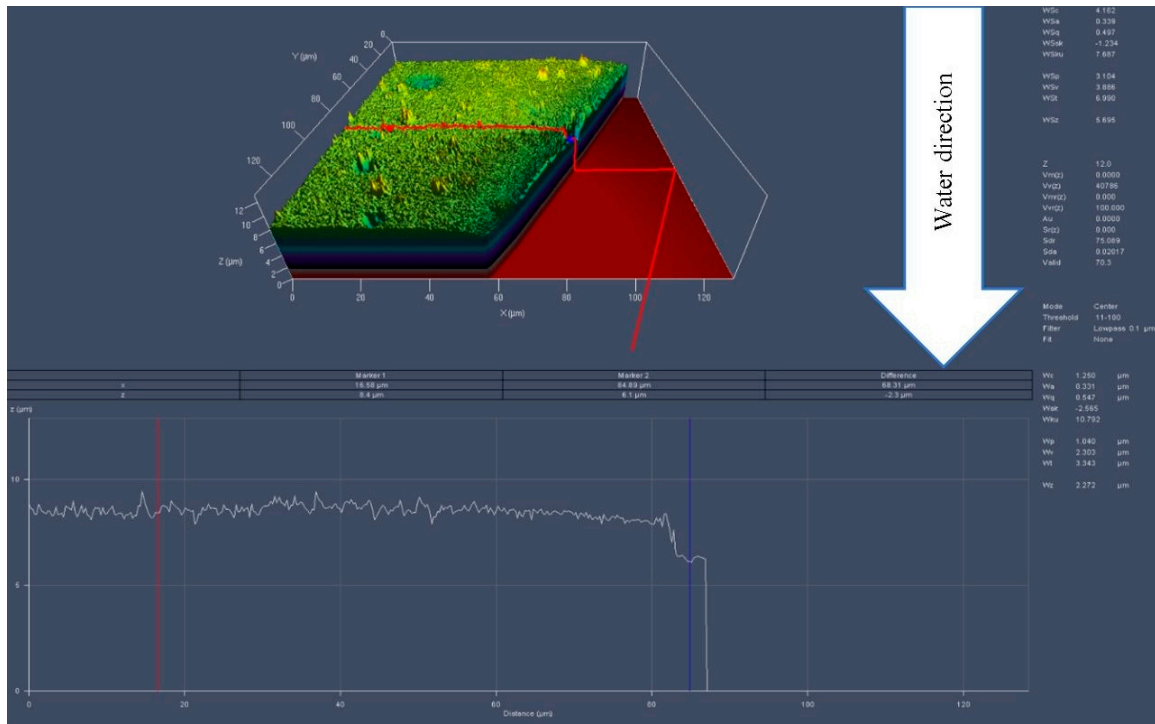


Figure 12. Surface topography of sample X2 after operation; red line—measuring line.

In the examination of cavitation generator X1, we identified notable issues concerning the long axial coating detachment and delamination along the edge of the working opening. The cavitation wear observed exhibited a distinct polygonal shape, with varying heights across the constructional element, as well as voids (cavities) resulting from the removal of tungsten carbides. Figure 13a,b illustrate these significant findings. Additionally, we detected cavitation wear effects near the straight-through openings, which are presented as brittle cracks and delamination, resulting in a mesh pattern of the WC/C coating across extensive areas of the sample. Alarming, as the cracked coating shifted toward the working opening during operation, gaps formed between the individual plates of the WC/C coating. This concerning progression ultimately led to the complete detachment from the substrate, causing larger fragments to disintegrate under the influence of the high-pressure medium. Addressing these challenges is crucial for enhancing the durability and effectiveness of the cavitation generator.

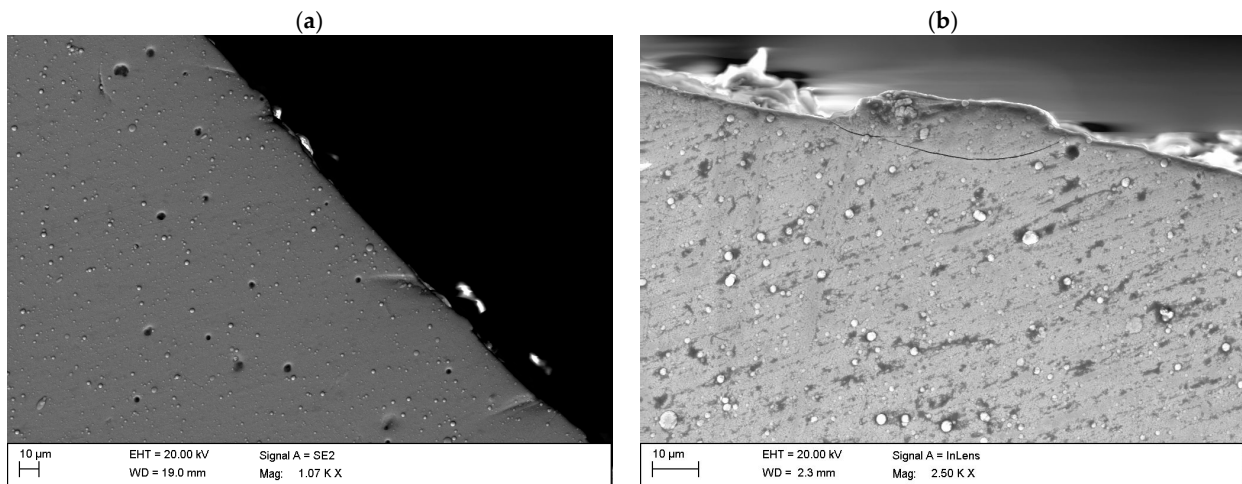


Figure 13. (a,b) Result of cavitation wear of the surface of sample X1 after operation.

Figure 14 clearly illustrates surface fatigue wear characterized by unidirectional brittle cracks. These cracks result from overlapping cyclic cavitation stresses, which lead to micro-deformations and micro-cracks in the top layer of the CrN + WC/C coating. The initiation of these fractures occurs in regions where tungsten carbide droplets have been removed, particularly at the craters and cavitation cavities. The cracks in the coating propagate axially toward the edge of the working hole, causing notable chipping and detachment of the coating material. Additionally, the examined fragments of the structural element's surface, as presented in Figure 14, reveal numerous voids, craters, and cavitation cavities that resulted from the removal of tungsten carbide droplets. These features are direct consequences of the cyclic-stress cavitation processes associated with flowing water, especially pronounced around the edges and near the working straight-through hole (Figure 14a).

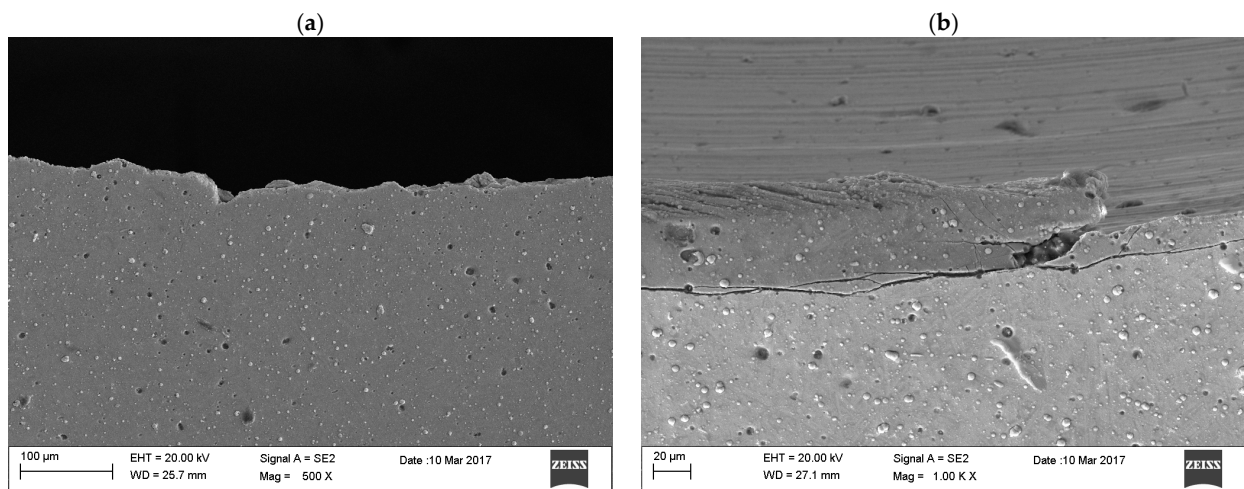


Figure 14. (a,b) Effects of cavitation wear of the surface of sample X2.

4. Conclusions

Based on the tests carried out in the closed-cycle continuous flow device, which generate a cavitation environment, both with cavitation generators without protective coatings and with WC/C and/or CrN + WC/C coatings applied with various PVD methods, the following was found:

- Despite the use of corrosion-resistant steels, which include steels from the group X2CrNi18-9, as a result of the cavitation environment, this causes surface material wear, especially in the area of the through holes. At the hole boundaries of cavitation generators, few cracks in the coatings were found. This is due to the fact that there are no protective coatings inside the through hole; thus, there is no continuity of the coating.
- The use of protective coatings WC/C and/or CrN + WC/C protects both the surface of the cavitation generators, as well as the places most exposed to wear in the area of the through holes. Using the appropriate coatings will significantly extend the life of such a generator and, thus, reduce the costs associated with replacing the cavitation generator and reducing the efficiency of this type of device.
- Through an X-ray phase analysis of cavitation generators with WC/C and CrN + WC/C coatings, the austenitic crystal structure of the X-ray substrate in the form of γ -iron was confirmed. Furthermore, it is also possible to identify on the diagrams, for all the studied samples, a broad/fuzzy diffraction line, the so-called broadening, which is the result of the diffraction of the X-ray beam on the amorphous structure, in the angular range between $35 \div 50^\circ 2\theta$ (Figure 5). The amorphous nature of the

WC/C and CrN + WC/C coatings was also confirmed by diffraction methods using a transmission electron microscope (Figure 9). An unambiguous confirmation of the structure of both the substrate and the applied PVD coatings was provided by structural and diffraction studies of the thin films, which confirmed that the structure of the samples designated as X1 and X2 are characterized by an austenitic structure.

- Based on the results of the surface topography studies before and after the operation of PVD-coated cavitation generators operating in a flow-blasting device, brittle cracks and the detachment of parts of the material were observed, especially in the areas near the edge, towards the inside of the through hole, due to the influence of long-term cyclic-fatigue processes occurring in the coating, as well as in the steel substrate itself.
- In further studies, the authors of this paper will focus on the application of other types of protective coatings, primarily CVD coatings, which will allow for the tight protection of the entire surface of the cavitation generator, including, in particular, the through holes, which have been proven to be the main point of initiation of cavitation damage processes.
- Based on the conducted operational tests in an environment of intensive cavitation wear of cavitation generators made of X2CrNi18-9 steel with WC/C and CrN + WC/C protective coatings, it was found that, for the tested steel with multilayer CrN + WC/C coatings, there were significantly fewer cavitation defects both on the surface of the material and on the edge of through holes, which indicates that the use of these multilayer coatings can significantly extend the service life of structural elements operating in such environmental conditions.

Author Contributions: Methodology, T.L. and P.S.; Validation, T.T.; Writing—original draft, W.B.; Writing—review & editing, T.L. and P.S.; Supervision, T.T. All authors have read and agreed to the published version of the manuscript.

Funding: This research received no external funding.

Institutional Review Board Statement: Not applicable.

Informed Consent Statement: Not applicable.

Data Availability Statement: The original contributions presented in this study are included in the article. Further inquiries can be directed to the corresponding author.

Conflicts of Interest: Tomasz Linek was employed by the company Cerrad Sp. z o.o. The remaining authors declare that the research was conducted in the absence of any commercial or financial relationships that could be construed as a potential conflict of interest.

References

1. Liu, X.; Zhang, L. Friction and wear behaviors of engineering materials: A review. *Wear* **2020**, *3*, 446–447.
2. Koziej, A.; Weroński, A. Kawitacja elementów układu przepływowego pomp wodociagowych. *Inż. Mater.* **2007**, *6*, 920–924.
3. Krella, A. Cavitation erosion of TiN and CrN coatings deposited on different substrates. *Wear* **2013**, *297*, 992–997. [[CrossRef](#)]
4. Luo, X.; Ji, B.; Tsujimoto, Y. A review of cavitation in hydraulic machinery. *J. Hydrodyn.* **2016**, *28*, 335–358. [[CrossRef](#)]
5. Stachowiak, G.W.; Batchelor, A.W. *Engineering Tribology*, 4th ed.; Butterworth-Heinemann: Oxford, UK, 2014.
6. Koziej, A. Zużycie kawitacyjne elementów układu przepływowego poziomych zespołów pompowych niskiego ciśnienia na przykładzie stacji wodociagowej. *Nauka Tech. Eksploat. Niezawodn.* **2004**, *2*, 32–35.
7. Korniyenko, A. Method for Producing Heat for Heating Building and Constructions and a Continuous Cavitation Heat Generator. European Patent EP 1706679 B1, 3 December 2008.
8. Faes, W.; Lecompte, S.; Ahmed, Z.; Van Bael, J.; Salenbien, R.; Verbeken, K.; De Paepe, M. Corrosion and corrosion prevention in heat exchangers. *Corros. Rev.* **2019**, *37*, 131–155. [[CrossRef](#)]
9. Karimi, Z.; Sadeghi, A.; Ghaffarinejad, A. The comparison of different deposition methods to prepare thin film of silicon-based anodes and their performances in Li-ion batteries. *J. Energy Storage* **2023**, *72 Pt A*, 108282. [[CrossRef](#)]

10. Krella, A. The new parameter to assess cavitation erosion resistance of hard PVD coatings. *Eng. Fail. Anal.* **2011**, *18*, 855–867. [[CrossRef](#)]
11. Krella, A. Degradacja powłok CrN osadzonych na stalowe podłoża w warunkach oddziaływania kawitacji. *Inż. Mater.* **2013**, *34*, 110–115.
12. Czyżniewski, A.; Krella, A. Wytwarzanie i właściwości powłok TiN i CrN w zastosowaniu do ograniczenia zużycia elementów maszyn przez kawitację. *Inż. Mater.* **2006**, *27*, 360–363.
13. Heathcook, C.J.; Protheroe, B.E.; Ball, A. Cavitation erosion of stainless steels. *Wear* **1982**, *81*, 311–327. [[CrossRef](#)]
14. Ghiban, B.; Bordeasu, I.; Ghiban, N.; Badarau, R.; Hadar, A.; Serban, N. Some aspects of cavitation damages in austenitic stainless steels. *Ann. DAAAM Proc.* **2008**, 541–543.
15. Wang, Z.; Zhu, J. Correlation of martensitic transformation and surface mechanical behavior with cavitation erosion resistance for some iron-based alloys. *Wear* **2004**, *256*, 1208–1213. [[CrossRef](#)]
16. Zylla, I.-M.; Hougardy, H.P. Cavitation behavior of metastable Cr-Mn-austenite. *Steel Res.* **1994**, *65*, 132–170. [[CrossRef](#)]
17. Kumar, S.; Brennen, C.E. A study of pressure pulses generated by travelling bubble cavitation. *J. Fluid Mech.* **1993**, *255*, 541–564. [[CrossRef](#)]
18. Brennen, C.E. *Cavitation and Bubble Dynamics*; Cambridge University Press: New York, NY, USA, 2014; p. 68.
19. Stachowiak, G.W.; Batchelor, A.W. Cavitation wear. In *Engineering Tribology*; Tribology Series; Butterworth-Heinemann: Oxford, UK, 1993; Volume 24, pp. 1–872.
20. Ki-Han, K.; Chahine, G.; Franc, J.-P.; Karimi, A. (Eds.) *Advanced Experimental and Numerical Techniques for Cavitation Erosion Prediction*; Springer: Dordrecht, The Netherlands, 2014.
21. Karimi, A.; Avellan, F. Comparison of Erosion Mechanisms in Different Types of Cavitation. *Wear* **1986**, *113*, 305–322. [[CrossRef](#)]
22. Tanski, T.; Labisz, K.; Borek, W.; Staszuk, M.; Brytan, Z.; Krzeminski, Ł. Application of the Finite Element Method for Modelling of the Spatial Distribution of Residual Stresses in Hybrid Surface Layers. In *Mechanical and Materials Engineering of Modern Structure and Component Design*; Advanced Structured Materials; Springer: Cham, Switzerland, 2015; Volume 70, pp. 51–69.
23. Linek, T.; Tański, T.; Borek, W. Influence of surface roughness on the cavitation wear of P265GH and X2CrNi18-9 steel cavitation generators. *Communications* **2018**, *20*, 48–54. [[CrossRef](#)]
24. Linek, T. Effects of Applying WC/C Protective Coating on Structural Elements Working in Cavitation Environment. In *Cavitation*; IntechOpen: London, UK, 2018; pp. 7–27.
25. Linek, T.; Tański, T.; Borek, W. Comparison of wear of applied CrN+WC/C and WC/C and protective coatings operating under cavitation environment. In Proceedings of the 24th International Seminar of Ph.D. Students SEMDOK 2019, Zuberec, Slovakia, 30 January–1 February 2019.
26. Borek, W.; Linek, T.; Tański, T.; Staszuk, M.; Pancielejko, M. Mechanical and Functional Properties of Cavitation Generators with PVD Functional Coatings Intended for Use in the Cavitation Environment. *Key Eng. Mater.* **2019**, *813*, 234–240. [[CrossRef](#)]

Disclaimer/Publisher’s Note: The statements, opinions and data contained in all publications are solely those of the individual author(s) and contributor(s) and not of MDPI and/or the editor(s). MDPI and/or the editor(s) disclaim responsibility for any injury to people or property resulting from any ideas, methods, instructions or products referred to in the content.